

## Albumin Is a Substrate of Human Chymase

PREDICTION BY COMBINATORIAL PEPTIDE SCREENING AND DEVELOPMENT OF A SELECTIVE INHIBITOR BASED ON THE ALBUMIN CLEAVAGE SITE\*

Received for publication, April 18, 2003, and in revised form, June 9, 2003  
Published, JBC Papers in Press, June 18, 2003, DOI 10.1074/jbc.M304087200

Wilfred W. Raymond, Sandra Waugh Ruggles, Charles S. Craik, and George H. Caughey‡

From the Cardiovascular Research Institute and Departments of Medicine and Pharmaceutical Chemistry, University of California at San Francisco, San Francisco, California 94143-0911

Human chymase is a chymotryptic serine peptidase stored and secreted by mast cells. Compared with other chymotryptic enzymes, such as cathepsin G and chymotrypsin, it is much more slowly inhibited by serum serpins. Although chymase hydrolyzes several peptides and proteins *in vitro*, its target repertoire is limited compared with chymotrypsin because of selective interactions in an extended substrate-binding site. The best-known natural substrate, angiotensin I, is cleaved to generate vasoactive angiotensin II. Selectivity of angiotensin cleavage depends in major part on interactions involving substrate residues on the carboxyl-terminal (P1'–P2') side of the cleaved bond. To identify new targets based on interactions with residues on the amino-terminal (P4–P1) side of the site of hydrolysis, we profiled substrate preferences of recombinant human chymase using a combinatorial, fluorogenic peptide substrate library. Data base queries using the peptide (Arg-Glu-Thr-Tyr-X) generated from the most preferred amino acid at each subsite identify albumin as the sole, soluble, human extracellular protein containing this sequence. We validate the prediction that this site is chymase-susceptible by showing that chymase hydrolyzes albumin uniquely at the predicted location, with the resulting fragments remaining disulfide-linked. The site of hydrolysis is highly conserved in vertebrate albumins and is near predicted sites of metal cation binding, but nicking by chymase does not alter binding of  $\text{Cu}^{2+}$  or  $\text{Zn}^{2+}$ . A synthetic peptidic inhibitor, diphenyl *N*<sup>α</sup>-benzoxycarbonyl-L-Arg-Glu-Thr-Phe<sup>P</sup>-phosphonate, was designed from the preferred P4–P1 substrate sequence. This inhibitor is highly potent (IC<sub>50</sub> 3.8 nM) and 2,700- and 1,300-fold selective for chymase over cathepsin G and chymotrypsin, respectively. In summary, these findings reveal albumin to be a substrate for chymase and identify a potentially useful new chymase inhibitor.

cretory granules in certain human mast cell subpopulations that are particularly concentrated in skin (6, 7). Active chymase is released from stimulated mast cells along with histamine, heparin, and tryptases (8). Secreted chymase is inhibited by  $\alpha_1$ -antichymotrypsin and other circulating antipeptidases (9, 10). However, this inhibition is slow compared with that of other chymotryptic peptidases, such as chymotrypsin and cathepsin G (9). Consequently, chymase retains activity long enough after release to find and cleave extracellular targets. For example, chymase is the major extravascular source of vasoactive angiotensin II (11, 12), which is generated with exceptional efficiency by human chymase via hydrolysis of the Phe-8–His-9 bond of angiotensin I (13, 14). A variety of other peptide and protein targets of chymase are proposed, based primarily on *in vitro* studies. These include bradykinin (15), C1 inhibitor (16), interleukin-1 $\beta$  (17), neurotensin (18), procollagen and procollagenase (19, 20), kit ligand (21), endothelins (22), and profilins (23) (see Table I). The range of potential plasma-derived targets is large, especially in settings of vascular leakage provoked by co-released mast cell histamine. However, the most important biological function of human chymase remains to be established with certainty; indeed, physiologically relevant targets may remain to be identified.

In chymase, as in other trypsin-family serine peptidases, key substrate binding interactions occur in an active site cleft formed between two, six-stranded  $\beta$ -barrel domains (24, 25). Differences in substrate specificity among individual members of this large family of peptidases arise from variations in the surface topography of amino acid backbone and side chains lining the substrate-binding cleft. The enzyme active site can be divided into a series of subsites interacting with particular substrate residues. In reference to the peptide substrate, we use standard nomenclature (26), with peptide bond amidolysis occurring between P1 and P1' in theoretical substrate Pn . . . P3, P2, P1, P1', P2', P3' . . . Pn', where each P is an amino acid. The most critical interaction occurs in the primary specificity pocket, which accommodates the side chain of the P1 amino acid. This side chain is aromatic for chymases and other chymotryptic enzymes. In the case of chymase-mediated hydrolysis of angiotensin I, interactions involving P1, P1', and P2' are particularly important (24, 25, 27, 28). However, for many serine peptidases (including chymase and cathepsin G hydrolyzing other peptide substrates), interactions on the other side of P1 (involving P4, P3, and P2) critically influence substrate binding and hydrolysis (29, 30). In the current work, we probe the substrate preferences of human chymase at P4–P1 using a combinatorial substrate library containing most combinations of natural amino acids at each subsite position. The results successfully predict chymase-mediated hydrolysis of a new pro-

Chymases are chymotryptic serine peptidases expressed principally by mast cells (1). Although several chymases are transcribed and translated from a family of closely linked genes in rodents (2, 3), there appears to be just one chymase gene (*CMAI*) in humans (4, 5). Abundant chymase is stored in se-

\* This work was supported in part by National Institutes of Health Grants HL-24136 (to W. W. R. and G. H. C.) and CA72006 (to S. W. R. and C. S. K.). The costs of publication of this article were defrayed in part by the payment of page charges. This article must therefore be hereby marked "advertisement" in accordance with 18 U.S.C. Section 1734 solely to indicate this fact.

‡ To whom correspondence should be addressed. Tel.: 415-476-9920; Fax: 415-476-9749; E-mail: ghc@itsa.ucsf.edu.

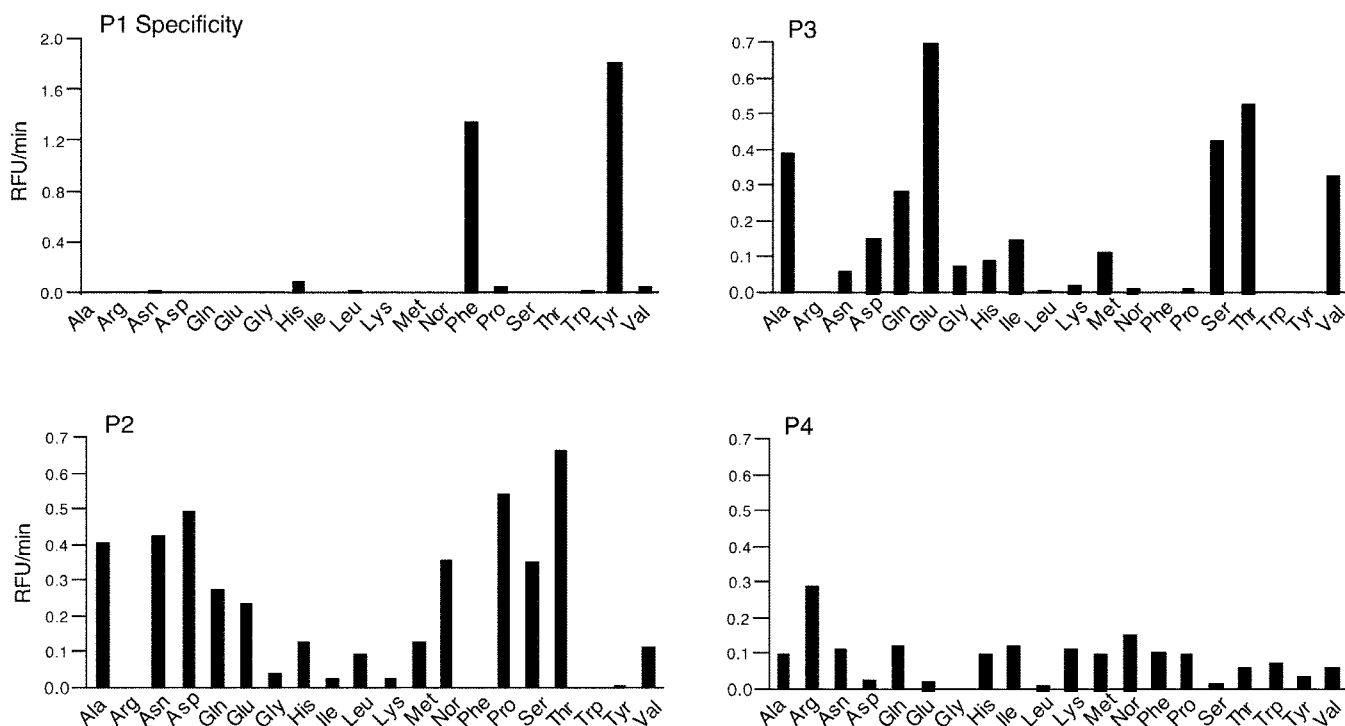


FIG. 1. **Subsite preferences of human chymase.** Purified, recombinant  $\alpha$ -chymase was profiled using libraries of fluorogenic tetrapeptide substrates. Primary specificity was tested in a library in which each of the designated 20 amino acids was held constant in turn as residues P2 through P4 were varied among the 20 amino acids. Therefore, each assay condition tested a mixture of 8,000 different peptide substrates for a given P1 residue. Chymase-mediated substrate hydrolysis liberated the fluorogenic leaving group 7-amino-4-carbamoylmethylcoumarin. Readout was in relative fluorescence units (RFU) per min. As shown in the “P1 specificity” panel, chymase greatly prefers substrates with P1 Tyr or Phe. The other three panels show results of similar profiling of preferences at positions P2, P3, and P4, respectively, by fixing amino acids at the designated position and varying the residues at the remaining three positions. Although a range of amino acids was preferred or tolerated at positions P2–P4, the single best predicted tetrapeptide substrate sequence is Arg-Glu-Thr-Tyr, a sequence found naturally in human albumin.

TABLE I  
Sites of hydrolysis of natural targets of human chymase

Target	P4–P1	Citations
Albumin	RETY	This work
Angiotensin I	IHPF and DRVY (minor)	(13, 14)
C1 inhibitor	KMLF	(16)
Endothelin-1	VVPY	(22)
Human chymase	PSQF	(11)
Procollagenase	QFVL	(20)
Interleukin 1 $\beta$	NEAY	(17)
Neurotensin	RRPY	(18)
Kit ligand	TKPF	(21)
Bradykinin	FSPF	(15)
Birch profilin	WQTY & GSVW	(23)
Human profilin	PSVW	(23)
Procollagen 1 $\alpha$	LKSL	(19)
Macroglobulin	RVGF and VGFY	(10)

tein target, human serum albumin (HSA).<sup>1</sup> A synthetic, peptidic inhibitor based on this cleavage site is a potent, selective inhibitor of chymase.

#### EXPERIMENTAL PROCEDURES

**Expression, Purification, and Activation of Recombinant Human Chymase**—For the studies described in this report, we generated recombinant human (rh) prochymase in insect (*Trichoplusia ni*) cells as previously described (14). Briefly, rhprochymase was purified by high performance heparin-affinity chromatography and then activated by incubation with dipeptidylpeptidase I. The activated preparation was

repurified by heparin-affinity chromatography to remove dipeptidylpeptidase. The repurified enzyme was pure by SDS-PAGE and amino-terminal sequence analysis and was highly active, with a specific activity of 177  $\mu\text{mol min}^{-1} \text{mg}^{-1}$  versus succinyl-L-Ala-Ala-Pro-Phe-4-nitroanilide (suc-AAPF-NA; Sigma) under standard conditions (14). This activity closely matches that of native human chymase tested under identical substrate and assay conditions (9).

**Screening with Combinatorial, Fluorogenic Peptide Libraries**—To profile rhchymase preferences at substrate positions P4–P1, we followed the general approaches described previously for selected other serine peptidases (31, 32), including chymotrypsin. Briefly, to probe the influence of the P1 residue, we used rhchymase to screen a P1-diverse library of soluble positional protease substrates with 160,000 members, each containing the fluorogenic leaving group 7-amino-4-carbamoylmethylcoumarin. This library contains substrate amino acid diversity at positions P4, P3, P2, P1 (31), with each position varying in 20 amino acids (omitting Cys and adding Ile). The P1-diverse library consists of 20 wells, in each of which only the P1 residue remains constant, with each of the remaining sites containing equimolar mixtures of 20 amino acids for a total of 8,000 sequences per well. Similarly, the extended P4–P2 specificity of rhchymase was explored by fixing the residue at the desired position in a given well. Assays were performed at 25 °C in 50 mM Tris (pH 8.0), 100 mM NaCl, 0.01% Tween 20, and 1% Me<sub>2</sub>SO. Final concentration for each substrate compound was 10 nM. Substrate hydrolysis was initiated by addition of enzyme (10 nM) and monitored fluorometrically with excitation at 380 nm and emission at 450 nm.

**Molecular Modeling of Human Chymase with a Predicted Best Substrate**—We used SwissModel and SwisspdbViewer software (33) to model the best substrate identified by combinatorial screening. The starting point for the model was the crystal-based structure of rhchymase bound to (and inactivated by) suc-AAPF-chloromethylketone (25), which attaches covalently to chymase’s active site histidine. The suc-AAP moiety was exchanged for residues P4, P3, P2 of the identified best substrate.

**Incubation of Albumin with Chymotryptic Peptidases and Identification of Sites of Hydrolysis**—Recombinant chymase was incubated with HSA (enzyme to substrate molar ratio of 1:83) at 37 °C in PBS. The source of HSA was fraction V albumin (Sigma). The latter was further

<sup>1</sup> The abbreviations used are: HSA, human serum albumin; rh, recombinant human; PBS, phosphate-buffered saline; 5-Br-PAPS, 2-(5-bromo-2-pyridylazo)-5-(*N*-*n*-propyl-*N*-(3-sulfopropyl)amino) phenol; RETY, Arg-Glu-Thr-Tyr; Z-RETf-(OPh)<sub>2</sub>, diphenyl *N*<sup>α</sup>-benzoxycarbonyl-L-Arg-Glu-Thr-Phe<sup>P</sup>-phosphonate; MeOsc-AAPF-(OPh)<sub>2</sub>, diphenyl *N*<sup>α</sup>-methoxysuccinyl-L-Ala-Ala-Pro-Phe<sup>P</sup>-phosphonate; suc-AAPF-NA, succinyl- *N*<sup>α</sup>-L-Ala-Ala-Pro-Phe-4-nitroanilide.

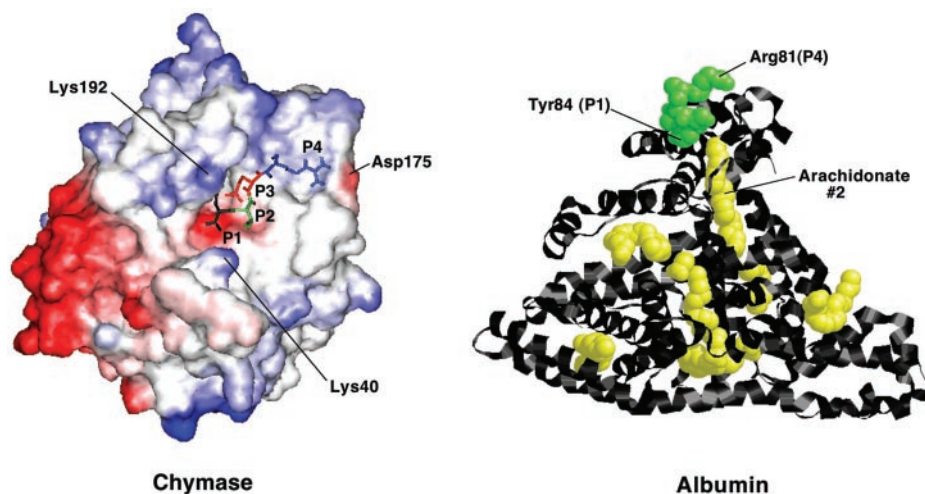


**FIG. 2. Molecular models of chymase and albumin.** The chymase model in the *left panel* is based on the crystallographically derived coordinates of human chymase model 1ppj. Using SwissModel, residues P4–P2 of the bound inhibitor in 1ppj were replaced with residues P4–P2 (Arg-Glu-Thr) of our best substrate, as predicted by results of screening with the combinatorial peptide library. In this rendering, the chymase surface is electrostatically contoured, with concentrations of positive charge shown in *blue* and areas of surface negative charge in *red*. The P1 residue is attached covalently to chymase's active site His. The P1 aromatic side chain is deeply buried and only partly visible beneath Lys-192, as indicated. The tip of P4 Arg's positively charged guanidinium group is positioned to interact with the negatively charged side chain of Asp-175, as indicated. Similarly, the P3 Glu side chain carboxylate can interact favorably with the  $\epsilon$  amino group of Lys-192 as indicated but is too remote from Lys-40 to interact with the side chain of that residue. The side chain of P2 Thr in part faces solvent and in part contacts the neutral to slightly acidic bed of the substrate-binding site adjacent to the site of catalysis. Thus, electrostatic complementarities as well as other contacts appear to favor interactions between residues P4–P2 of the model peptide and the chymase active site. The model shown in the *right panel* is based on structure 1gnj, which derives from HSA co-crystallized with arachidonate (34). In this view, the three-cornered helical protein structure of HSA is rendered mostly in *black ribbons*. The site of hydrolysis by chymase is Tyr-84, which is depicted in *green*, space-filling mode, along with the other residues comprising the chymase recognition sequence: Arg-81-Glu-82-Thr-83. To facilitate comparison, residues P4–P1 of the cleavage site in HSA and of the model peptide in the chymase active site in the adjacent panel are oriented similarly. For the sake of contrast, the seven embedded arachidonates of HSA are shown in *yellow*. The arachidonate closest to the site of proteolysis is No. 2, as indicated. The amino terminus of the protein can be seen on the *top right edge* of the structure. It should be noted that 1gnj does not reveal any sites of metal cation binding and in fact lacks HSA's first two amino-terminal residues (Asp-Ala), which can ligand  $\text{Cu}^{2+}$ . The scale of the HSA model is smaller than that of chymase, which is about half the size of HSA.

purified by high performance anion exchange chromatography (MonoQ column; Amersham Biosciences) to remove traces of impurities such as serpin-class serine peptidase inhibitors. The reaction was quenched by boiling in SDS-PAGE sample buffer and the products of hydrolysis subjected to reducing and non-reducing SDS-PAGE. To establish the rate of hydrolysis, 5 pmol of chymase were incubated with 1 nmol of HSA in 50  $\mu\text{l}$  of PBS at 37  $^{\circ}\text{C}$ . At various times, aliquots were removed and chymase inactivated by addition of glacial acetic acid. Products were separated by reducing SDS-PAGE. Coomassie Blue-stained bands were quantitated by densitometry. In separate experiments, chymase-cleaved HSA was electrophoresed and blotted to polyvinylidene difluoride membrane. The larger of the two new bands generated by chymase was excised and sequenced from the amino terminus by Edman degradation (Midwest Analytical, St. Louis, MO). To compare effects of chymase with those of other chymotryptic peptidases, HSA was incubated in parallel experiments with human cathepsin G (Elastin Products, St. Louis, MO) and bovine  $\alpha$ -chymotrypsin (Sigma) using amounts of enzyme producing equal rates of hydrolysis of suc-AAPF-NA under similar conditions.

**Molecular Modeling of Albumin**—To model HSA in the vicinity of the chymase hydrolysis site, we used the RasMol molecular visualization program and an x-ray diffraction-derived structure of HSA co-crystallized with arachidonate (Protein Data Bank identifier 1gnj; Ref. 34).

**Analysis of Metal Cation Binding to Albumin**—We evaluated the effect of chymase cleavage of HSA on  $\text{Zn}^{2+}$  and  $\text{Cu}^{2+}$  binding by competitive spectrophotometry (35). Unbound  $\text{Zn}^{2+}$  or  $\text{Cu}^{2+}$  in a solution of HSA was detected using a metal-binding indicator ligand, 2-(5-bromo-2-pyridylazo)-5-(*N-n*-propyl-*N*-(3-sulfopropyl)amino)phenol (5-Br-PAPS; Dojindo Laboratories, Kumamoto, Japan), which competes with HSA for metal cations and changes spectrally when bound to  $\text{Zn}^{2+}$ , as described in Ref. 35. Briefly, 2.5–7.5  $\mu\text{M}$  HSA in 20 mM Tris-HCl (pH 7.0) and 150 mM NaCl was incubated for 1 h at 37  $^{\circ}\text{C}$  with or without 70 nM rhchymase followed by addition of 10  $\mu\text{M}$  5-Br-PAPS. Change in absorbance at 446 nm was measured after each of six sequential additions of  $\text{ZnSO}_4$  in 0.5- $\mu\text{M}$  increments. Measurements without HSA also were made to assess binding of  $\text{Zn}^{2+}$  to 5-Br-PAPS in the absence of competitor. After these determinations, samples containing HSA were analyzed by SDS-PAGE to assess extent of cleavage by chymase. The

effect of hydrolysis of HSA on binding to  $\text{Cu}^{2+}$  was assessed similarly.

**Testing of Peptide-based Chymase Inhibitors**—A diphenyl phosphonate ester transition-state analog inhibitor based on the best tetrapeptide substrate identified by combinatorial screening of the substrate library was obtained from Enzyme Systems Products (Livermore, CA). This inhibitor, diphenyl *N* $^{\alpha}$ -benzoxycarbonyl-L-Arg-Glu-Thr-Phe<sup>P</sup>-phosphonate (Z-RETF-(OPh)<sub>2</sub>) was constructed with an analog of Phe rather than Tyr at the P1 position for ease of synthesis. As shown under "Results," Phe is nearly as favored as Tyr in the combinatorial screening assay. Performance of this inhibitor was compared with that of a traditional chymase inhibitor, diphenyl *N* $^{\alpha}$ -methoxysuccinyl-L-Ala-Ala-Pro-Phe<sup>P</sup>-phosphonate (MeOsuc-AAPF-(OPh)<sub>2</sub>) and with diphenyl phosphonates based on a series of Phe-based, chloromethylketone-class chymase inhibitors reported by Hayashi *et al.* (36). The series used here includes benzoyl-L-Phe<sup>P</sup>-(OPh)<sub>2</sub>, 2-phenyl-acetyl-Phe<sup>P</sup>-(OPh)<sub>2</sub>, 3-phenyl-propionyl-Phe<sup>P</sup>-(OPh)<sub>2</sub>, and 4-phenyl-butryl-Phe<sup>P</sup>-(OPh)<sub>2</sub> and were obtained from Enzyme Systems Products. The concentration of diphenyl phosphonate producing 50% inhibition ( $\text{IC}_{50}$ ) of rhchymase, cathepsin G, and  $\alpha$ -chymotrypsin was determined for each of the compounds at an enzyme concentration of 0.5 nM using the chromogenic substrate suc-AAPF-NA (0.2 mM). The effects of Z-RETF-(OPh)<sub>2</sub> and MeOsuc-AAPF-(OPh)<sub>2</sub> were tested in two buffer conditions, standard "high-salt" chymase assay buffer (0.45 M Tris-HCl, pH 8, 1.8 M NaCl, 9% Me<sub>2</sub>SO) (9) and PBS (pH 7.4) with 10% Me<sub>2</sub>SO.

## RESULTS AND DISCUSSION

**P1 Subsite Preferences Predicted by the Combinatorial Substrate Library**—As shown in Fig. 1, the combinatorial peptide screen finds the most striking preferences at the P1 position in comparison with positions P2–P4, with Tyr slightly preferred over Phe. All other P1 choices are a distant second. Unlike cathepsin G, a related serine peptidase with chymotryptic activity that is co-expressed with chymase in human mast cells (37, 38) and duodenases, which are expressed in ruminant mast cells (39), human chymase lacks "dual specificity," *i.e.* an ability to hydrolyze both tryptic and chymotryptic substrates.

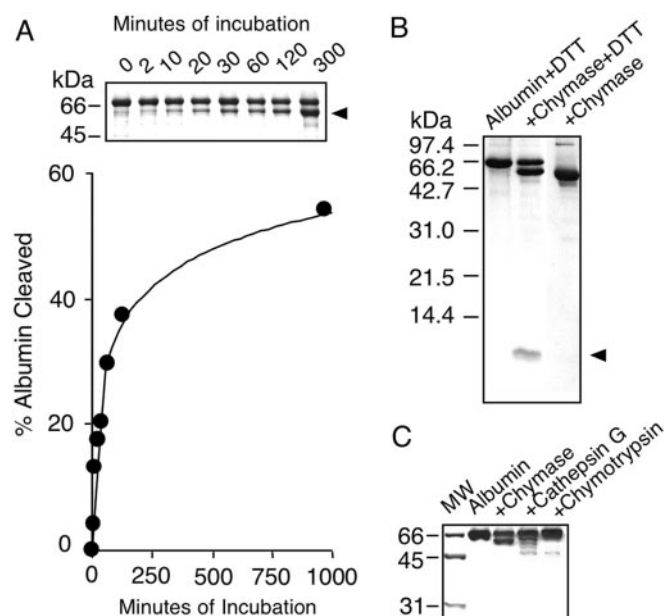


**FIG. 3. Hydrolysis of albumin by chymotryptic proteases.** *A*, time-dependent hydrolysis of HSA by chymase. Recombinant human chymase (1 nM) was incubated with 20  $\mu$ M HSA (enzyme/substrate ratio of 1:20,000). Samples withdrawn at intervals as indicated were subjected to reducing SDS-PAGE and stained with Coomassie Blue. As shown in the representative electrophoretogram, the parent band progressively disappears with a concomitant increase in a lower band of  $\sim$ 59 kDa, as indicated by the *triangle* to the *right* of the figure. The size (in kDa) and elution positions of marker proteins are shown to the *left*. The *graph* shows densitometric analysis of the hydrolysis events shown in the *top part* of the panel. The data indicate that chymase hydrolyzes HSA predominantly at a single site and that the initially rapid rate of hydrolysis declines exponentially over time. *B*, comparison of the electrophoretic behavior of chymase-hydrolyzed HSA with and without reduction with dithiothreitol (DTT). The *first two lanes* contain DTT-reduced HSA before and after incubation with chymase. The *third lane* contains unreduced, chymase-cleaved HSA, which migrates somewhat faster than reduced, uncleaved HSA. The *arrowhead* identifies the position of the chymase-generated small fragment, which is evident only in reduced material. The positions of DTT-treated marker proteins are indicated. These data indicate that fragments of HSA remain disulfide-linked after being clipped by chymase. *C*, comparison of HSA cleavage by chymase, cathepsin G, and chymotrypsin. This electrophoretogram shows results of separate incubations of HSA with each of three chymotryptic enzymes. The lane marked *MW* contains marker proteins, the size (in kDa) of which is indicated to the *left* of the figure. The adjacent lane contains HSA incubated in buffer alone. The other lanes contain HSA incubated with chymase, cathepsin G, and chymotrypsin, as indicated. Amounts of each enzyme were equal in hydrolyzing suc-AAPF-NA, a standard chymotryptic substrate. Under these conditions, chymase achieves  $\sim$ 50% hydrolysis, primarily at a single site. Cathepsin G (which has tryptic as well as chymotryptic activity) also produces some fragmentation but at multiple sites. Chymotrypsin does little compared with chymase. The major fragments generated by cathepsin G and chymotrypsin differ from those generated by chymase. Thus, chymase is a more potent and selective albuminase than the other two major chymotryptic serine peptidases.

There is only a small tendency to cleave fluorogenic substrates with P1 Trp or Leu. This contrasts with preferences of pancreatic chymotrypsin tested in the same system (31), which reveals a proportionately much higher ability to hydrolyze substrates with P1 Trp and Leu. The limited affinity of chymase for substrates with these P1 residues perhaps is explained by characteristics of the so-called primary specificity pocket, as assessed in crystallized versions of the human enzyme (24, 25). This pocket may be too small to accommodate the indole side chain of Trp easily but too large to develop strong binding interactions with the aliphatic side chain of Leu. Nonetheless, as shown in Table I, Trp or Leu does occupy the P1 site in some targets of human chymase. However, P1 is Tyr or Phe in a

generous majority of identified natural substrates. It is worth noting that targets hydrolyzed by chymase at P1 Trp (profilins) and P1 Leu (procollagen and procollagenase) are large proteins. In the case of profilin, the vulnerable P1 Trp appears to be exposed on the protein surface (23). Such exposure may be as important in determining the ability of chymase to hydrolyze a target as the subsite preferences under study here. Presumably, many uncleaved target sequences in proteins would be cleaved by chymases if they were incorporated into peptides rather than buried in the hydrophobic interior of the protein, as is the case for most aromatic amino acids in globular proteins.

**P2–P4 Subsite Preferences**—As shown in Fig. 1, there is little tolerance for aromatic or basic residues at either P2 or P3. However, a variety of hydrophilic, neutral, and acidic amino acids are accepted at P2, the best being Thr. The P3 position, unlike P2, tolerates Pro poorly and prefers Glu slightly to several other acceptable amino acids. Finally, at the P4 subsite, Arg is preferred about 2-fold over any other choice. Acidic residues (Asp and Glu) are poor, and Gly is worst. Note that effects of the best residues in positions P2–P4 on substrate cleavage rate is generally much less than that of the P1 Phe and Tyr residues, hence the differences in scale in the graphs depicted in Fig. 1. Overall, the restricted range of preferences for each position can be summarized as follows: P4, Xaa (slightly Arg); P3, Glu/Ser/Thr; P2, Thr/Pro; P1, Tyr/Phe. A consensus substrate based on the single most preferred amino acid at each position is Arg-Glu-Thr-Tyr (RETY).

**Comparison with Prior Efforts to Profile the Chymase Active Site**—Aside from a finding that P1 Phe is slightly preferred over Tyr in selected nitroanilide substrates, our data are consistent with prior results obtained with panels of peptidyl 4-NAs varying at P1 (29). As was predicted previously in a selected series of peptidyl 4-NAs (29), Pro is one of the most favored P2 residues, although this preference is uncommon among proteases, including others profiled with combinatorial, fluorogenic substrates (31, 32). However, the best P2 residue identified by our profiling method is Thr, a finding that did not emerge from previous attempts to characterize preferences at this subsite. The relative intolerance of P3 for aromatic residues in our study contrasts somewhat with the study by Powers *et al.* (29), who found suc-L-Phe-Pro-Phe-4-NA to be a good substrate, although not as good as otherwise identical substrates with a sampling of neutral/aliphatic, hydrophilic, or acidic residue at P3. In our study, the P3 preference for Glu and intolerance of Pro agrees with a study by Bastos *et al.* (40) of non-cleavable chymase inhibitors. Differences between our study and those of Powers *et al.* in part may be because of differences in the length of the peptide or in the identity of the leaving group. We studied tetrapeptides with 7-amino-4-carbamoylmethylcoumarin as the leaving group, whereas Powers *et al.* studied succinylated tripeptides with 4-NA as the leaving group. Also, the profiling of subsites P2 and P3 by Powers *et al.* was carried out almost exclusively with Phe in the P1 position, whereas our characterization was carried out in mixtures of substrates with 20 different amino acids at P1. Furthermore, their characterization at P2 was carried out with P3 fixed at Phe and the characterization of P3 with P2 fixed at Pro. It also should be emphasized that any non-additive interactions, favorable or unfavorable, between substrate residues occupying different subsite positions will tend to make an individual substrate appear more or less acceptable in comparison to the suitability predicted from mixtures of peptides, as in our study. The possibility of such interactions between subsites is suggested by a study of a library of non-cleavable, peptidic inhibitors of chymase (40) as well as by studies of chymase-mediated hydrolysis of angiotensin analogs (27). The observed effect of

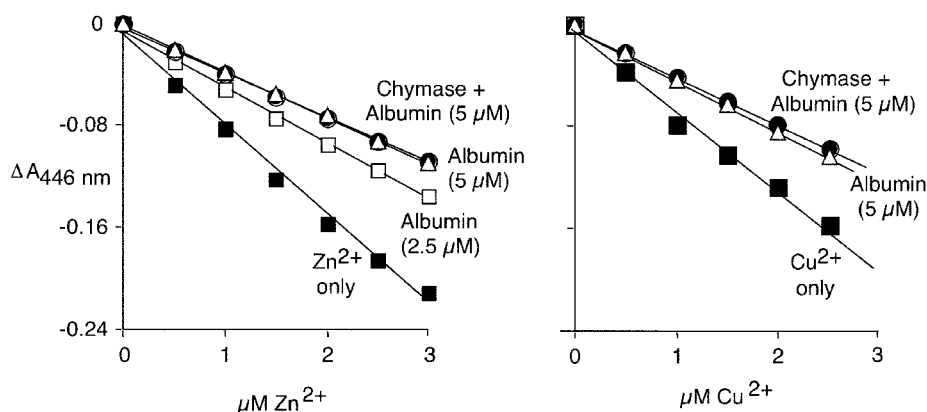


FIG. 4. **Binding of metals to chymase-cleaved albumin.** Binding of  $Zn^{2+}$  and  $Cu^{2+}$  to HSA was analyzed by competitive spectrophotometry. These metal cations are thought to occupy different sites in HSA. Binding of these ions to 5-Br-PAPS decreases its absorbance at 446 nm in a concentration-dependent manner. Binding of metals by HSA precludes binding to 5-Br-PAPS, thereby preventing the decrease in absorbance. The *left* and *right panels* show the effects of HSA on 5-Br-PAPS binding of  $Zn^{2+}$  and  $Cu^{2+}$ , respectively. The observed  $\Delta A_{446}$  is linear over the range of metal concentrations and varies with HSA concentration, indicating that the assay is capable of detecting drops in competitive binding of metals at these HSA concentrations. However, as shown by the *black circles*, hydrolysis by chymase neither increases nor decreases the ability of HSA to compete with 5-Br-PAPS for binding of  $Zn^{2+}$  or  $Cu^{2+}$ . Thus, hydrolysis by chymase has no major effect on binding by these divalent metal cations.

P4 amino acids with an acidic side chain is consistent with prior results obtained using a limited series of tetrapeptidyl 4-nitroanilides (not including P4 Arg, Asp, or Gly) in which Glu was found to be the least favorable of examined P4 residues (29). The unfavorable effect of an acidic moiety at P4 may have globally reduced the binding affinity of the Powers series of tripeptidyl 4-NAs, all of which contain P4 succinate as an  $\alpha$ -amino blocking group (29). Our consensus-preferred substrate, RETY, differs in all four positions from the consensus best substrate predicted from panels of 4-NAs, but there is general agreement about the categories of amino acids that are favored or accepted at each position. In chymase's most extensively characterized natural peptide target, angiotensin I, which is hydrolyzed at Phe-8 with a P4–P1 sequence of Ile-His-Pro-Phe, our consensus substrate also disagrees at all positions, perhaps in part reflecting the potential influence of P' residues in substrate binding. Overall, however, as shown in Fig. 1, each of the angiotensin residues is favored or acceptable at each position.

**Modeling of RETY in the Active Site of Human Chymase**—As shown in Fig. 2A, the consensus-preferred substrate predicted by our combinatorial peptide screening approach is readily accommodated in the human chymase active site, replacing the suc-L-Ala-Ala-Pro-(Phe) of 1pjp, in which the P1 Phe derivative is covalently attached to the imidazole side chain of the catalytic triad histidine (25). The phenolic side chain of predicted P1 Tyr fits easily into the primary specificity pocket. The hydrophilic side chain of P2 faces largely toward solvent but the main chain, as well as parts of the side chain, does contact several residues on the active site floor (see Fig. 2). On the other hand, our model indicates that the acidic side chain of P3 Glu can interact favorably with the basic tip of chymase's Lys-192, which forms part of the wall of the active site cleft as well as part of the ceiling of the deep hydrophobic pocket accommodating the substrate P1 aromatic side chain. This wall is poorly formed in prochymase, which has 7,000-fold diminished catalytic activity compared with the mature enzyme (41). Our model also indicates that substrate P4 Arg's guanidinium moiety can interact electrostatically with the side chain carboxylate of chymase's Asp-175.

**Data Base Screening Suggests That Human Albumin Is a Potential Target**—The strongest test of the utility of a profiling strategy is the ability to identify natural substrates that were

not previously considered. In a screen of the Protein Data Base of crystallized proteins using the consensus RETY query sequence, the only human protein identified was HSA. From the more extensive Swissprot data base, several additional human proteins were identified, mainly intracellular proteins or membrane proteins with a target sequence in a cytoplasmic domain. These are unlikely targets of a secreted peptidase. A possible exception is multimerin, a multidomain, secreted (but cell surface-bound) protein of unknown function produced by platelets and vascular endothelial cells (42). Multimerin is a potential target in cases of vascular disruption, when mast cells and platelets might come into close contact. It should be noted that the predicted site of cleavage by chymase in multimerin is near the predicted site of cell attachment and would not be expected to shed the major fragment from the cell surface. HSA is even more attractive as a potential target of chymase because it is abundant (35–50 g/liter in plasma) and should be highly available to secreted chymase, especially in the context of histamine-induced vascular leakage. Also, HSA is essential for maintaining colloid osmotic pressure (thereby preventing tissue edema) and is a major transport agent for metals, lipids, and drugs (reviewed in Ref. 43). Thus, alteration or destruction of HSA could have functional consequences.

**Limited Hydrolysis of Albumin by Chymase**—Characterization of HSA after incubation with chymase confirms our prediction that it is a substrate. As shown in Fig. 3, chymase generates an  $\sim 59$ -kDa fragment from HSA (after reduction), plus a  $<10$ -kDa fragment migrating close to the dye front, indicating a single major site of hydrolysis. Edman degradation of the amino terminus of the  $\sim 59$ -kDa fragment reveals the sequence Gly-Glu-Met-Ala-Asp, which is the sequence that would be generated by hydrolysis at Tyr-84. Thus, of numerous potential chymotryptic hydrolysis sites in HSA (a protein of 585 amino acids with 46 Phe or Tyr residues in the mature protein), only one is cleaved with notable avidity in the natively folded protein. This P4–P1 sequence of this site matches our "best substrate," RETY. It should be noted that HSA, which has an average circulating life of 27 days (43), generally resists degradation. Although chymase generates two fragments of HSA when the products are subjected to SDS-PAGE under reducing conditions, no fragmentation occurs under non-reducing conditions (Fig. 3B). This suggests that the fragments remain disulfide-linked after proteolysis by chymase and supports the pro-

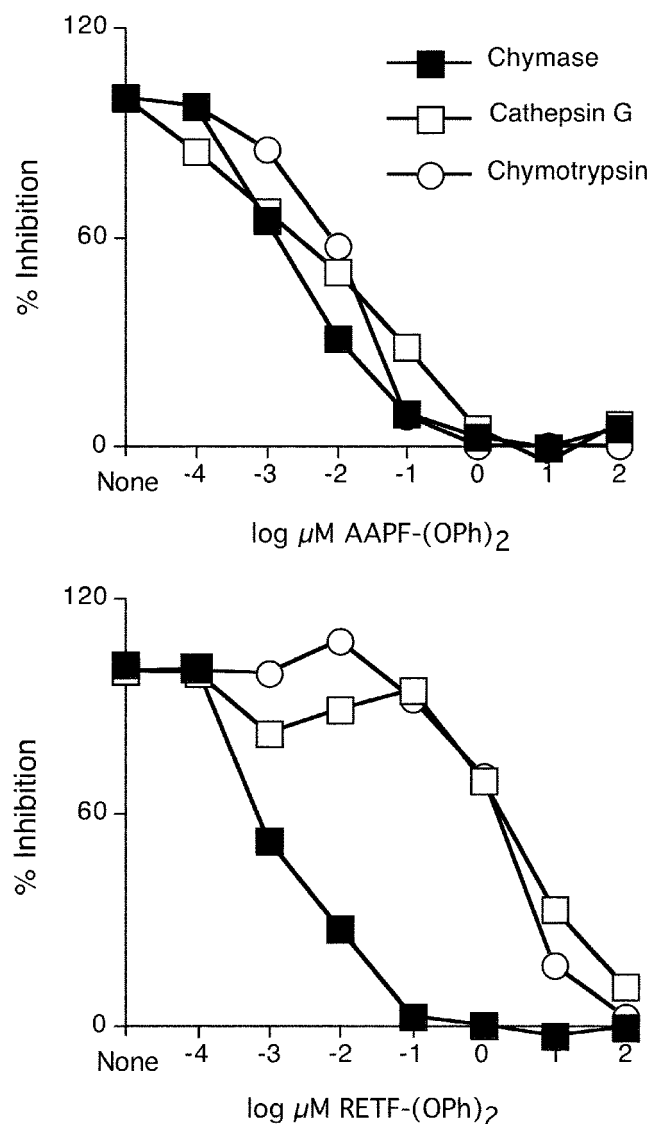


**FIG. 5. Inhibition of chymotryptic serine peptidases by peptidic diphenyl phosphonates.** Chymase, cathepsin G, and chymotrypsin were incubated with a range of concentrations of the standard diphenyl phosphonate inhibitor of chymotryptic peptidases, MeOsuc-AAPF-(OPh)<sub>2</sub>, and with a novel diphenyl phosphonate compound, Z-RETF-(OPh)<sub>2</sub>, which was constructed based on results of screening of chymase in the combinatorial substrate library. The *top* and *bottom* panels show representative inhibition curves for MeOsuc-AAPF-(OPh)<sub>2</sub> and Z-RETF-(OPh)<sub>2</sub>, respectively. Percent inhibition is calculated as percentage of activity relative to that measured in the absence of inhibitor. The IC<sub>50</sub> for each enzyme (see Table II) was determined by extrapolation. Note that MeOsuc-AAPF-(OPh)<sub>2</sub> is a potent but non-selective inhibitor of all three chymotryptic peptidases. Z-RETF-(OPh)<sub>2</sub> is even more potent in inactivating chymase (with an IC<sub>50</sub> of ~1 nM in this experiment) but is over three orders of magnitude less active toward cathepsin G and chymotrypsin. Thus, Z-RETF-(OPh)<sub>2</sub> is a strong and highly selective inhibitor of human chymase.

posed linkage between Cys-75 and Cys-90 suggested by crystallographic and other data (34). The persistent covalent linkage after hydrolysis also predicts that chymase will not alter the role of the cleaved protein in maintaining colloid osmotic pressure because the linked fragments will retain the same oncotic activity. Chymase is a potent albuminase under our conditions, generating hydrolytic fragments at enzyme/substrate ratios of 1:20,000 or less. Hydrolysis is time-dependent, as shown in Fig. 3A, with the reaction slowing over time, consistent with possible product inhibition. Based on initial rates of hydrolysis determined from the experiments shown in

Fig. 3A, chymase cleaves HSA with a specific activity of 13 μmol (0.91 g) of HSA min<sup>-1</sup> per mg of active enzyme under our assay conditions, with one molecule of chymase hydrolyzing 6.8 molecules of HSA per second. These rates are achieved at HSA concentration of 20 μM, which is below the typical serum HSA level of ~0.8 mM. Our assays were conducted at concentrations of substrate below *K<sub>m</sub>* of HSA, which we are not able to establish because of the sensitivity limits of the electrophoretic assay and interference by trace amounts of chymase inhibitors at high concentrations of purified HSA. Compared with cathepsin G and chymotrypsin, chymase is a more selective and potent albuminase. As shown by the electrophoretogram in Fig. 3C, cathepsin G generates several light-staining fragments not seen in HSA incubated with chymase or chymotrypsin. This is consistent with prior studies indicating that cathepsin G is weaker than the other two enzymes toward most chymotryptic substrates (29) while possessing a unique "dual specificity" manifested in an ability to hydrolyze tryptic substrates with P1 basic residues (38). The pattern of cathepsin G-induced fragmentation seen in Fig. 3C is consistent with slow hydrolysis at multiple sites. Chymotrypsin, on the other hand, has little albuminase activity and does not generate products corresponding to the 59-kDa chymase-generated fragment.

*The Site of Chymase-mediated Hydrolysis in a Molecular Model of Albumin*—As shown in Fig. 2, the site of chymase-mediated cleavage at Tyr-84 is exposed on the surface, based on an x-ray diffraction-derived model of HSA (Protein Data Bank identifier 1gnj; Ref. 34). The chymase hydrolysis site forms a portion of the roof of just one of multiple identified sites of binding of arachidonate (34). However, none of the atoms involved in the RETY target sequence contacts an arachidonate, so it is unlikely that hydrolysis by chymase would have a major effect on lipid carriage by HSA. Indeed, the loop in HSA containing Tyr-84 is part of a short (14-amino acid) segment between disulfide anchors, with the carboxyl-terminal portion of the segment doubly anchored by tandem Cys residues (Cys-90 and -91), each participating in a different Cys-Cys linkage. Thus, the Tyr-84 loop is anchored by two disulfide linkages, which can minimize the disturbance to HSA's overall tertiary structure of chymase-mediated hydrolysis. It is perhaps relevant that the RETY target sequence is strongly conserved among mammals, being identical in humans, macaques, cows, and sheep (GenBank™ accession numbers AF542069, Q28522, P02769, X17055, respectively). Even chicken (*Gallus gallus*) albumin (X60688) is highly homologous (RDSY) in this region, with an acidic residue at P3 and a small hydrophilic residue at P2. The requirement for Glu or Asp at P3 and Tyr at P1 appears to be universal because it is present in all sequenced serum albumins, including salamander (AF217183). There are a variety of potential reasons that this sequence has been conserved through hundreds of millions of years of evolution. At present, there is insufficient correlation between albumin structure and function in this region to distinguish among the possibilities. However, it is tempting to speculate that this region offers a kind of "bait" to chymase.

*Effect of Chymase-mediated Hydrolysis of Albumin on Binding of Cu<sup>2+</sup> and Zn<sup>2+</sup>*—As shown in Fig. 4, the ability of chymase-cleaved HSA to compete with 5-Br-PAPS in binding to Zn<sup>2+</sup> or Cu<sup>2+</sup> is indistinguishable from that of native HSA. Thus, there is no major effect of cleavage by chymase on the strength of HSA's interactions with these metal cations. This is further evidence of the lack of major disturbances in HSA structure after cleavage by chymase. The site or sites of Zn<sup>2+</sup> binding is not known, but it differs from that of Cu<sup>2+</sup> and Ni<sup>2+</sup>, which are chelated by the first 3–4 amino acids of the amino terminus of HSA (44, 45). As shown by the model in Fig. 2, this

TABLE II  
Inhibition of chymotryptic enzymes by alkane phosphonates

Compound	IC <sub>50</sub> (μM) <sup>a</sup>		
	Chymase	Cathepsin G	Chymotrypsin
Z-RETF <sup>P</sup> -(OPh) <sub>2</sub>			
PBS <sup>b</sup>	0.0038 ± 0.0022	10.3 ± 7.3	4.8 ± 0.9
High-NaCl <sup>c</sup>	0.046 ± 0.011	5.6 ± 1.3	2.9 ± 1.0
MeOsuc-AAPF <sup>P</sup> -(OPh) <sub>2</sub>			
PBS <sup>b</sup>	0.0076 ± 0.024	0.040 ± 0.003	0.023 ± 0.020
High-NaCl <sup>c</sup>	0.024 ± 0.019	0.076 ± 0.006	0.043 ± 0.011
Benzoyl-F <sup>P</sup> -(OPh) <sub>2</sub>	8.9	8.6	ND <sup>d</sup>
2-Phenyl-acetyl-F <sup>P</sup> -(OPh) <sub>2</sub>	1.1	5.2	ND
3-Phenyl-propionyl-F <sup>P</sup> -(OPh) <sub>2</sub>	3.5	10.9	ND
4-Phenyl-butyryl-F <sup>P</sup> -(OPh) <sub>2</sub>	0.50	7.7	ND

<sup>a</sup> Substrate for all assays is suc-AAPF-4-nitroanilide (0.2 mM); enzymes are 0.5 nM.

<sup>b</sup> Assays carried out in PBS (pH 7.4), with 10% Me<sub>2</sub>SO.

<sup>c</sup> Assays carried out in Tris-HCl (pH 8), 1.8 M NaCl, 9% Me<sub>2</sub>SO.

<sup>d</sup> Not determined. Assays carried out in duplicate in high-NaCl buffer for the last four inhibitors.

amino terminus is near but not immediately adjacent to the site of hydrolysis by chymase. Thus, lack of an effect of HSA hydrolysis by chymase on Cu<sup>2+</sup> binding is consistent with prior hypotheses concerning the site of such binding derived from behavior of HSA-based model peptides and other data (44, 45).

*A New Inhibitor Based on the Albumin Cleavage Site Is a Potent and Selective Inhibitor of Chymase*—Fig. 5 compares concentration-inhibition curves for the standard chymase inhibitor MeOsuc-AAPF-(OPh)<sub>2</sub> with those of the novel compound Z-RETF-(OPh)<sub>2</sub> versus chymase, cathepsin G, and chymotrypsin. The IC<sub>50</sub> of Z-RETF-(OPh)<sub>2</sub>, which is based on HSA's site of cleavage by chymase, is compared with IC<sub>50</sub>s of additional diphenyl phosphonate chymase inhibitors in Table II. The data reveal that Z-RETF-(OPh)<sub>2</sub> is more potent than any of the other P1 Phe-based inhibitors in the series, including the standard chymase/cathepsin G inhibitor MeOsuc-AAPF-(OPh)<sub>2</sub>. This difference in potency is particularly striking in comparison with benzoyl-L-Phe<sup>P</sup>-(OPh)<sub>2</sub>, 2-phenyl-acetyl-Phe<sup>P</sup>-(OPh)<sub>2</sub>, 3-phenyl-propionyl-Phe<sup>P</sup>-(OPh)<sub>2</sub>, and 4-phenyl-butyryl-Phe<sup>P</sup>-(OPh)<sub>2</sub>. In comparison with MeOsuc-AAPF-(OPh)<sub>2</sub>, the most striking advantage of Z-RETF-(OPh)<sub>2</sub> is its selectivity for chymase. The selectivity differential is evident in both PBS and high-NaCl buffer but is dramatic in the former, with a 2,710- and 1,270-fold difference in IC<sub>50</sub> between chymase versus cathepsin G and chymotrypsin, respectively. The diminished selectivity of Z-RETF-(OPh)<sub>2</sub> in buffer of high ionic strength presumably stems from interference with electrostatic interactions between substrate Arg and Glu side chains and chymase that are more productive at physiological ionic strength of PBS. As shown in Fig. 2, the substrate P4 Arg and P3 Glu side chains, respectively, can interact with acidic and basic side chains of catalytic domain amino acids of the extended substrate-binding site of chymase. These favorable electrostatic contacts appear to be unavailable to RETF in modeled homologous regions of cathepsin G and chymotrypsin (not shown), as one might also predict from failure of inhibitor performance to improve at low ionic strength in PBS (in which IC<sub>50</sub>s actually increase; see Table II). Thus, these data suggest specifically that P4 and P3 residues of Z-RETF-(OPh)<sub>2</sub> may make large contributions to inhibitor selectivity. More generally, the data suggest that substrate assay conditions can substantially influence performance characteristics of peptidic inhibitors. By contrast, MeOsuc-AAPF-(OPh)<sub>2</sub>, which is neutral to hydrophobic, is nonselective with regard to inactivation of the three major chymotryptic enzymes. Moreover, its performance varies minimally with buffer condition, suggesting that the differences in the two buffers do not intrinsically alter responses of these enzymes to phosphonate inhibitors. As expected, Z-RETF-(OPh)<sub>2</sub> does not inhibit tryptic or pancreatic serine

peptidases, *i.e.* human mast cell tryptase, bovine pancreatic trypsin, and porcine pancreatic elastase (IC<sub>50</sub> >100 μM; data not shown). Therefore, Z-RETF-(OPh)<sub>2</sub> is a potent and selective inhibitor of human chymase at the pH and ionic strength of extracellular fluids into which mast cells deposit their peptidases.

As a group, phosphonate inhibitors form stable complexes with serine peptidases by forging a covalent link with the active site Ser-195 Oγ and mimicking the tetrahedral intermediate formed by Ser-195 and substrate Cα at the scissile bond prior to hydrolytic release of cleaved fragments (46, 47). The O-phenyl groups of bound inhibitor dissociate in an "aging" process. Despite their active site reactivity, diphenyl phosphonate esters are chemically stable and thus may be useful *in vitro* and *in vivo* as pharmacological tools for probing chymase function.

#### REFERENCES

1. Caughey, G. H. (1998) in *Handbook of Proteolytic Enzymes* (Barrett, A. J., Rawlings, N., and Woessner, F., eds), pp. 66–79, Academic Press, London.
2. Gurish, M. F., Nadeau, J. H., Johnson, K. R., McNeil, H. P., Grattan, K. M., Austen, K. F., and Stevens, R. L. (1993) *J. Biol. Chem.* **268**, 11372–11379.
3. Huang, R., and Hellman, L. (1994) *Immunogenetics* **40**, 397–414.
4. Caughey, G. H., Zerweck, E. H., and Vanderslice, P. (1991) *J. Biol. Chem.* **266**, 12956–12963.
5. Caughey, G. H., Schaumburg, T. H., Zerweck, E. H., Butterfield, J. H., Hanson, R. D., Silverman, G. A., and Ley, T. J. (1993) *Genomics* **15**, 614–620.
6. Schechter, N. M., Fraki, J. E., Geesin, J. C., and Lazarus, G. S. (1983) *J. Biol. Chem.* **258**, 2973–2978.
7. Irani, A. A., Schechter, N. M., Craig, S. S., DeBlois, G., and Schwartz, L. B. (1986) *Proc. Natl. Acad. Sci. U. S. A.* **83**, 4464–4468.
8. Goldstein, S. M., Leong, J., Schwartz, L. B., and Cooke, D. (1992) *J. Immunol.* **148**, 2475–2482.
9. Schechter, N. M., Sprows, J. L., Schoenberger, O. L., Lazarus, G. S., Cooperman, B. S., and Rubin, H. (1989) *J. Biol. Chem.* **264**, 21308–21315.
10. Walter, M., Sutton, R. M., and Schechter, N. M. (1999) *Arch. Biochem. Biophys.* **368**, 276–284.
11. Urata, H., Kinoshita, A., Misono, K. S., Bumpus, F. M., and Husain, A. (1990) *J. Biol. Chem.* **265**, 22348–22357.
12. Balcells, E., Meng, Q. C., Johnson, W. H., Jr., Oparil, S., and Dell'Italia, L. J. (1997) *Am. J. Physiol.* **273**, H1769–H1774.
13. Reilly, C. F., Tewksbury, D. A., Schechter, N. B., and Travis, J. (1982) *J. Biol. Chem.* **257**, 8619–8622.
14. Caughey, G. H., Raymond, W. W., and Wolters, P. J. (2000) *Biochim. Biophys. Acta* **1480**, 245–257.
15. Reilly, C. F., Schechter, N. B., and Travis, J. (1985) *Biochem. Biophys. Res. Commun.* **127**, 443–449.
16. Schoenberger, O. L., Sprows, J. L., Schechter, N. M., Cooperman, B. S., and Rubin, H. (1989) *FEBS Lett.* **259**, 165–167.
17. Mizutani, H., Schechter, N., Lazarus, G., Black, R. A., and Kupper, T. S. (1991) *J. Exp. Med.* **174**, 821–825.
18. Kinoshita, A., Urata, H., Bumpus, F. M., and Husain, A. (1991) *J. Biol. Chem.* **266**, 19192–19197.
19. Kofford, M. W., Schwartz, L. B., Schechter, N. M., Yager, D. R., Diegelmann, R. F., and Graham, M. F. (1997) *J. Biol. Chem.* **272**, 7127–7131.
20. Saarinen, J., Kalkkinen, N., Welgus, H. G., and Kovanen, P. T. (1994) *J. Biol. Chem.* **269**, 18134–18140.
21. Longley, B. J., Tyrrell, L., Ma, Y., Williams, D. A., Halaban, R., Langley, K., Lu, H. S., and Schechter, N. M. (1997) *Proc. Natl. Acad. Sci. U. S. A.* **94**, 9017–9021.
22. Nakano, A., Kishi, F., Minami, K., Wakabayashi, H., Nakaya, Y., and Kido, H.

- (1997) *J. Immunol.* **159**, 1987–1992
23. Mellon, M. B., Frank, B. T., and Fang, K. C. (2002) *J. Immunol.* **168**, 290–297
24. McGrath, M. E., Mirzadegan, T., and Schmidt, B. F. (1997) *Biochemistry* **36**, 14318–14324
25. Pereira, P. J. B., Wang, Z. M., Rubin, H., Huber, R., Bode, W., Schechter, N. M., and Strobl, S. (1999) *J. Mol. Biol.* **286**, 163–173
26. Schechter, I., and Berger, A. (1968) *Biochem. Biophys. Res. Commun.* **32**, 898–902
27. Sanker, S., Chandrasekharan, U. M., Wilk, D., Glynias, M. J., Karnik, S. S., and Husain, A. (1997) *J. Biol. Chem.* **272**, 2963–2968
28. Muilenburg, D. J., Raymond, W. W., Wolters, P. J., and Caughey, G. H. (2002) *Biochim. Biophys. Acta* **1596**, 346–356
29. Powers, J. C., Tanaka, T., Harper, J. W., Minematsu, Y., Barker, L., Lincoln, D., Crumley, K. V., Fraki, J. E., Schechter, N. M., Lazarus, G. G., Nakajima, K., Nakashino, K., Neurath, H., and Woodbury, R. G. (1985) *Biochemistry* **24**, 2048–2058
30. Tanaka, T., Minematsu, Y., Reilly, C. F., Travis, J., and Powers, J. C. (1985) *Biochemistry* **24**, 2040–2047
31. Harris, J. L., Backes, B. J., Leonetti, F., Mahrus, S., Ellman, J. A., and Craik, C. S. (2000) *Proc. Natl. Acad. Sci. U. S. A.* **97**, 7754–7759
32. Harris, J. L., Niles, A., Burdick, K., Maffitt, M., Backes, B. J., Ellman, J. A., Kuntz, I., Haak-Frendscho, M., and Craik, C. S. (2001) *J. Biol. Chem.* **276**, 34941–34947
33. Peitsch, M. C. (1996) *Biochem. Soc. Trans.* **24**, 274–279
34. Petitpas, I., Grune, T., Bhattacharya, A. A., and Curry, S. (2001) *J. Mol. Biol.* **314**, 955–960
35. Ohyoshi, E., Hamada, Y., Nakata, K., and Kohata, S. (1999) *J. Inorg. Biochem.* **75**, 213–218
36. Hayashi, Y., Iijima, K., Katada, J., and Kiso, Y. (2000) *Bioorg. Med. Chem. Lett.* **10**, 199–201
37. Schechter, N. M., Irani, A. M., Sprows, J. L., Abernethy, J., Wintroub, B., and Schwartz, L. B. (1990) *J. Immunol.* **145**, 2652–2661
38. Polanowska, J., Krokoszynska, I., Czapinska, H., Watorek, W., Dadlez, M., and Otlewski, J. (1998) *Biochim. Biophys. Acta* **1386**, 189–198
39. Pemberton, A. D., Huntley, J. F., and Miller, H. R. (1997) *Biochem. J.* **321**, 665–670
40. Bastos, M., Maeji, N. J., and Abeles, R. H. (1995) *Proc. Natl. Acad. Sci. U. S. A.* **92**, 6738–6742
41. Reiling, K. K., Krucinski, J., Miercke, L. J., Raymond, W. W., Caughey, G. H., and Stroud, R. M. (2003) *Biochemistry* **42**, 2616–2624
42. Hayward, C. P., Hassell, J. A., Denomme, G. A., Rachubinski, R. A., Brown, C., and Kelton, J. G. (1995) *J. Biol. Chem.* **270**, 18246–18251
43. Peters, T. (1985) *Adv. Protein Chem.* **35**, 161–245
44. Carter, D. C., and Ho, J. X. (1994) *Adv. Protein Chem.* **45**, 153–203
45. Bar-Or, D., Curtis, G., Rao, N., Bampos, N., and Lau, E. (2001) *Eur. J. Biochem.* **268**, 42–47
46. Bone, R., Sampson, N. S., Bartlett, P. A., and Agard, D. A. (1991) *Biochemistry* **30**, 2263–2272
47. Bertrand, J. A., Oleksyszyn, J., Kam, C. M., Boduszek, B., Presnell, S., Plaskon, R. R., Suddath, F. L., Powers, J. C., and Williams, L. D. (1996) *Biochemistry* **35**, 3147–3155